Journal of Environmental Management 301 (2022) 113914

Contents lists available at ScienceDirect

Journal of Environmental Management

journal homepage: www.elsevier.com/locate/jenvman

Revealing the link between evolution of electron transfer capacity of humic acid and key enzyme activities during anaerobic digestion

Xiqing Wang [a], Tao Lyu [b], Renjie Dong [a], Shubiao Wu [c,*]

[a] Key Laboratory of Clean Utilization Technology for Renewable Energy, Ministry of Agriculture, College of Engineering, China Agricultural University, 100083, Beijing, PR China
[b] Cranfield Water Science Institute, Cranfield University, College Road, Cranfield, Bedfordshire, MK43 0AL, UK
[c] Department of Agroecology, Aarhus University, Blichers Allé 20, 8830, Tjele, Denmark

ARTICLE INFO

Keywords:
Anaerobic process
Anaerobic microbial community
Bio-waste management
Electron accepting/donating capacity
Humic substance

ABSTRACT

Humic acid (HA) is an important active compound formed during anaerobic digestion process, with a complex structure and dynamic electron transfer capacity (ETC). However, the mechanisms by which these macromolecular organic compounds dynamically interact with the microbial anaerobic digestion process at different operating temperatures are still unclear. In this study, the link between the evolution of the ETC of HAs and the microbial community under mesophilic and thermophilic conditions was investigated. The results showed an increasing trend in the ETC of HAs in both mesophilic (671–1479 μmol gHA^{-1}) and thermophilic (774–1506 μmol gHA^{-1}) anaerobic digestion (AD) until day 25. The ETC was positively correlated with the bacterial community of hydrolytic and acidogenic phases, but negatively correlated with the archaeal community of the methanogenic phase. Furthermore, the relationship between ETC and key enzyme activity was explored using a co-occurrence network analysis. HAs revealed a high potential to promote key enzyme activities during hydrolysis (amylase and protease) and acidification (acetate kinase, butyrate kinase, and phosphotransacetylase) while inhibiting the key enzyme activity in the methanogenic phase during the anaerobic digestion process. Moreover, HAs formed under thermophilic conditions had a greater influence on key enzyme activities than those formed under mesophilic conditions. This study advances our understanding of the mechanisms underlying the influence of HAs on anaerobic digestion performance.

1. Introduction

Anaerobic digestion (AD) is one of the effective treatments for the bioconversion of organic wastes to produce bioenergy of methane (Tang et al., 2018). In the AD process, organic matter is hydrolyzed into soluble organic units by a series of hydrolytic enzymes (e.g., amylase and protease), followed by the production of methane by transforming these compounds via acidogenic enzymes [e.g., acetate kinase (AK), butyrate kinase (BK), and phosphotransacetylase (PTA)] and methanogenic enzymes (e.g., F420-reducing hydrogenase) (Liu et al., 2015; Li et al., 2019a). Meanwhile, recalcitrant macromolecular organics, such as humic substances, are formed during the organic matter degradation and transformation processes (Wang et al., 2021a). Humic substances are mainly composed of humic acid, fulvic acid and humin (Guo et al., 2019). Among them, humic acid (HA), as one of the most important fractions of recalcitrant macromolecular organics, accounts for 14.6% of total solids and 27.0% of organic matter in the anaerobic digestion of sewage sludge (Tang et al., 2018). Meanwhile, HA content varies depending on the feeding materials and operational conditions (Wang et al., 2021a, 2021b). The content of HA ranged from 3.9 to 7.5 and 4.6–8.4 g L^{-1} during the mesophilic AD process with corn stover and chicken manure, respectively. Moreover, under the thermophilic condition, the content of HA ranged from 4.1 to 6.8 and 4.0–7.1 g L^{-1} during the corn stover and chicken manure, respectively.

Electron transfer capacity (ETC) is the dominant functional indicator of HAs in the remediation of inorganic or organic pollutants in contaminated environments, and it can be attributed to the strong potential of HAs to mediate biogeochemical redox reactions and accelerate the transformation of contaminants (Zhao et al., 2020). ETC can be described as the integrated function of electron accepting capacity (EAC) and electron donating capacity (EDC), which are closely correlated with the structural characteristics of HAs (Xiao et al., 2019). Previous studies have shown that the EDC of HAs positively correlates with

* Corresponding author.
E-mail address: wushubiao@agro.au.dk (S. Wu).

https://doi.org/10.1016/j.jenvman.2021.113914
Received 4 June 2021; Received in revised form 19 September 2021; Accepted 5 October 2021
Available online 7 October 2021

Nomenclature

AD	Anaerobic digestion
HA	Humic acid
ETC	Electron transfer capacity
EDC	Electron donating capacity
EAC	Electron accepting capacity
AK	acetate kinase
BK	butyrate kinase
PTA	phosphotransacetylase
F420	F420-reducing hydrogenase
HIX	Humification index
BIX	Biological index
DNS	Dinitrosalicylic acid

the phenolic group content (He et al., 2019), and the EAC positively correlates with the carboxyl group content (Aeschbacher et al., 2010; Xiao et al., 2019). Moreover, our previous findings showed that the evolution of HA structure during AD, with varying feeding materials and operating temperatures, greatly affected their ETCs and was closely associated with the methane production performance (Wang et al., 2021b).

The effect of HAs on AD performance has attracted attention in recent years, and the inhibitory effect of HAs on methane production has generally been concluded (Li et al., 2019a, 2019b). However, our previous findings illustrated that the influence of HAs on methane production is highly evolutionarily determined and may dynamically vary among different AD processes (Wang et al., 2021b). For example, the positive and negative effects of HAs on methane production were subsequently observed in the fast and slow methane production stages, respectively, owing to the concurrent decomposition and re-polymerization of HAs during AD. To date, the effect of HAs on AD has been mainly investigated by evaluating the methane production rates under varying external dosages of commercial HA analogs injected into anaerobic digesters (Li et al., 2014; Azman et al., 2017). Azman et al. (2017) reported that increasing levels of HA inhibited the hydrolysis efficiency of the cellulose and xylan anaerobic digestion by 40% and concomitantly reduced the methane yield. Likewise, other studies also indicated that after alkaline pretreatment and humic recovery, the biogas yield increased by 29.4–49.2% during subsequent sludge anaerobic digestion (Li et al., 2014). Nonetheless, considering methane as the product of a series of microbial-mediated reactions via action of multiple relatively key enzymes and microorganisms (Liu et al., 2015), current knowledge about the underlying mechanisms by which the dynamic evolution of the ETC of HAs interacts with these key enzymes and microbial communities is insufficient.

To fill this knowledge gap, a batch AD experiment with chicken manure under mesophilic and thermophilic conditions was performed. The objectives of the study were to explore the evolution of ETC of HAs and reveal the link between the ETCs of HAs and key enzyme activities in hydrolysis (amylase and protease), acidogenic (AK, BK, and PTA), and methanogenic (F420-reducing hydrogenase) phases using a co-occurrence network analysis. Our findings can help better understand the underlying mechanisms of the effect of HAs on AD performance.

2. Materials and methods

2.1. Batch AD experiments

Chicken manure has been well recognized in the world as a common representative substrate for AD plants. Batch AD of chicken manure under mesophilic and thermophilic conditions was performed. Briefly, chicken manure was collected from a biogas plant located in Beijing, China, and used as the feed material. Two types of sludge used as inoculums were obtained from two laboratory-scale mesophilic and thermophilic digesters, which were fed long-term with chicken manure. The total solids and volatile solid content of chicken manure and sludges were determined as per the standard methods (SCA, 2011). Briefly, the total solid was expressed as ratio of digestate weight before and after drying at 105 °C for 24 h when a steady mass was achieved. The volatile solid was measured by weight ratio of dried digestate before and after drying at 600 °C for 2 h until a steady mass was obtained. Then, the volatile solids content of chicken manure and the inoculum was 1:2, resulting in initial total solids and volatile solids of 6% (w/v %) and 3% (w/v %), respectively. The batch AD was incubated for 30 days at mesophilic (37 ± 1 °C) and thermophilic (55 ± 1 °C) conditions in a temperature-controlled incubator (RZH-380A, artificial climate chamber, China). Each treatment was performed in triplicate. The current study focuses on the potential relationship between the ETC of HAs and the key enzyme activities and microbial communities under different fermentation conditions. Samples from both systems were therefore collected on days 0, 5, 10, 15, 20, 25, and 30.

The performance of methane production has been reported in our previous study (Wang et al., 2021a, 2021b). Briefly, the yield methane rapidly achieved to 148 mL gVS^{-1} and 212 mL gVS^{-1} in day 10 under the mesophilic and thermophilic anaerobic digestion processes, respectively. Then, the methane generation gradually increased to 209 mL gVS^{-1} and 295 mL gVS^{-1} under the mesophilic and thermophilic conditions until day 30, respectively. Based on the theoretical Gompertz model, the methane generation process was categorised into two stages, i.e. fast and slow methane generation stages, with the turning point at day 10. Moreover, the volatile fatty acids, mainly in the short-chain fatty acids were determined via the Shimadzu CP3800 gas chromatography equipped with a DB-FFAP capillary column (30 m × 0.53 mm × 0.5 μm, Agilent Technologies, Inc., China) and a flame ionization detector. Further details on the analysis of the short-chain fatty acids can be found in Text S1 of the Supporting Information.

2.2. Microbial community analysis

The microbial communities of the samples from mesophilic and thermophilic digestions were analyzed using Illumina MiSeq sequencing. Briefly, total DNA extraction from samples was performed as described by Huang et al. (2021). 338F (50-ACTCCTACGGGAGG CAGCAG-30) and 806R (50-GGACTACHVGGGTW TCTAAT-30) were used as primers for bacterial analysis. The archaeal primers were Arch524F (50-TGYCAGCCGCCGCGGTAA-30) and Arch958R (50-YCCGGCGTTGAVTCCAATT-30). PCR was performed under the conditions described by Magdalena et al. (2021), and the products were analyzed on 2% agarose gels. Sequencing libraries were labeled with different multiplex indexing barcodes using the NEB Next Ultra DNA Library Prep Kit for Illumina (New England Biolabs Inc., USA) following the manufacturer's protocol. High-throughput sequencing analysis was performed on an Illumina MiSeq platform by Allwegene Technologies Co., Ltd. (Beijing, China). All sequence reads were clustered into operational taxonomic units (OTUs) using USEARCH (version 10.0, http://www.drive5.com/usearch/) and UCLUST (version 1.2, http://www.drive5.com/uclust/downloads1_2_22q.html), with a similarity threshold value of 97%.

2.3. Key enzyme activity analysis

The composition of chicken manure are carbohydrates, proteins, lipid, cellulose, lignin and hemicellulose (Provenzano et al., 2014; Bi et al, 2019a, 2019b; Rehman et al., 2017, 2019, 2019). Among them, the carbohydrates, proteins and lipid are the main compositions of chicken manure (Provenzano et al., 2014; Bi et al., 2019a, 2019b), where amylase and protease have been demonstrated as key enzymes contributing significantly to the transformation of such substances in the

hydrolysis phase (Chen et al., 2019). Therefore, the activity of amylase and protease were analyzed using the dinitrosalicylic acid (DNS) and L-lysine methods, respectively (Liu et al., 2015). The acetate kinase (AK), butyrate kinase (BK) and phosphotransacetylase (PTA) were the main acidogenic enzymes, and the F420-reducing hydrogenase was the key enzyme for methane generation. The activities of AK and BK were analyzed according to method described by Allen et al. (1964), and the activities of PTA and F420-reducing hydrogenase were analyzed following the method used by Trevors (1984). Moreover, AK, BK, PTA, and F420-reducing hydrogenase analysis kits (Lai Er Bio-Tech, Hefei, China) were used to analyze the activities of AK, BK, PTA, and F420-reducing hydrogenase, respectively. Before analysis, the digestates from mesophilic and thermophilic AD were washed with 100 mM phosphate buffer (PBS with pH of 7.4). Then, the digestates were sonicated at 4 °C for 30 min to break up the microbial cells and extract the enzymes sufficiently. Sonification was conducted with ultrasonic processor CPX 750 (Cole-Parmer Instrument, IL) at 20 kHz. The sonication lasted 30 min with one pause (2 min) every 5 min (Zhang et al., 2014). Finally, the supernatants were taken for analysis after centrifugation at 11000 rpm at 4 °C for 30 min.

2.4. HA characterization

The relative content and fluorescent parameters of HA were determined using excitation–emission matrix spectra combined with parallel factor (PARAFAC) analysis, as previously described by Wang et al. (2021b). Briefly, the fluorescence spectra of samples from mesophilic and thermophilic AD were first recorded using a fluorescence spectrophotometer (Aqualog, HORIBA) at emission and excitation wavelength ranges of 250–550 nm and 250–600 nm, respectively. Then, the PARAFAC was used to analyze the fluorescence spectra by using MATLAB R2018a (MathWorks, USA) with the DOMFluor Toolbox. Fluorescent parameters, including the humification index (HIX) and biological index (BIX), were calculated based on the excitation–emission matrix spectra.

The anaerobic digestate samples from each system were taken on days 0, 5, 10, 15, 20, 25, and 30. Prior to the structure and function analysis, the humic acids were extracted and purified according to the method reported by Zhao et al. (2020). The chemical composition (C, H, and N) of AD-derived HAs was characterized using elemental analysis (Vario EL cube, Germany). Fourier transform infrared (FTIR) spectra were measured from 4000 to 400 cm^{-1} at a resolution of 2 cm^{-1} using a Nicolet Nexus FTIR spectrophotometer (Thermo Nicolet Co., USA), as described by Tang et al. (2018). The ETCs, including EDC and EAC of HAs were measured using mediated electrochemical reduction and mediated electrochemical oxidation methods as described by Zheng et al. (2019). Briefly, the experiments were conducted on a Potentiostat workstation (CHI660D, Chenhua, Shanghai, China) with a counter electrode, reference electrode, and working electrode. The measurements were replicated three times to obtain reliable results.

2.5. Data analysis

Correlation analysis among the different parameters was conducted using SPSS software (version 22.0; IBM Corp., Armonk, NY, USA), and the graphs were plotted using Origin 8.5 (Origin Lab, USA). Visualized co-occurrence network figures were prepared using the Gephi 0.9.2 platform, as described by Lyu et al. (2018).

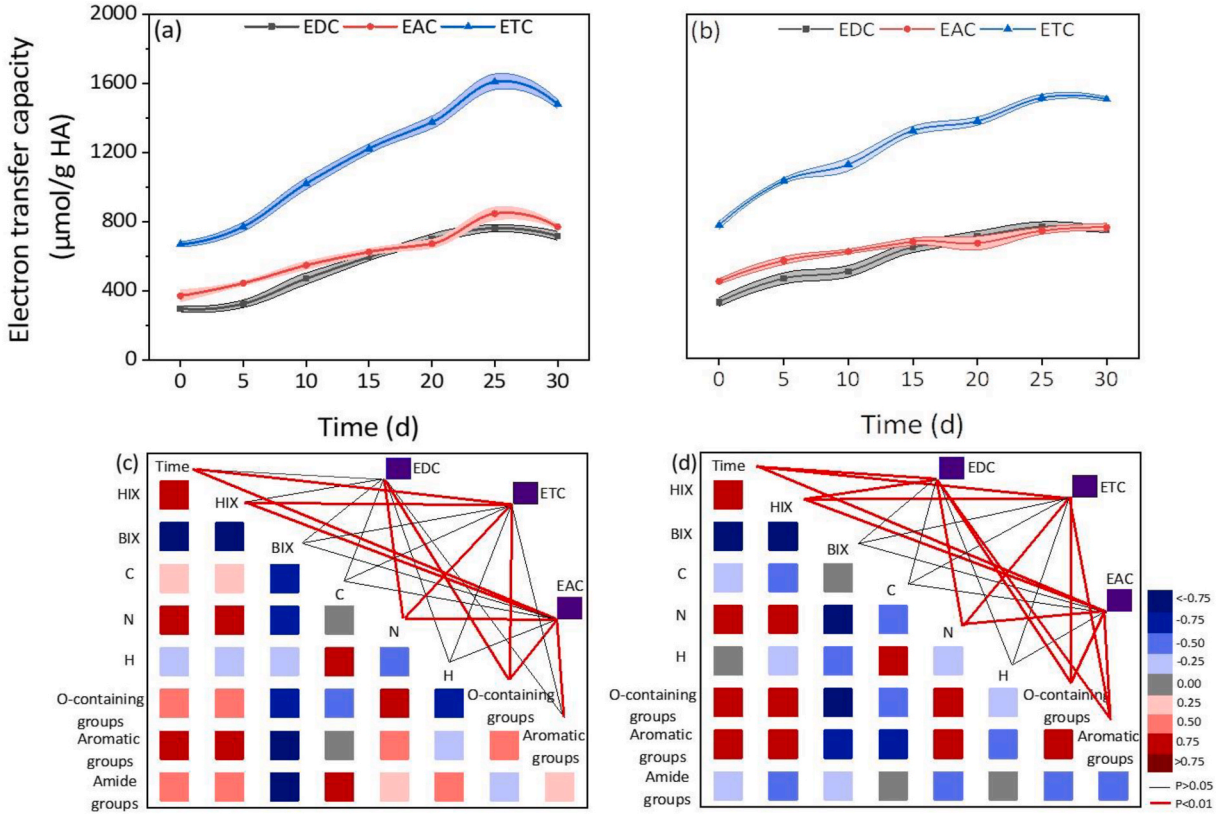

Fig. 1. Evolution of electron transfer capacity (ETC) during mesophilic (a) and thermophilic (b) anaerobic digestion. Correlation analysis between the ETC and chemical composition and structures of humic acid under mesophilic (c) and thermophilic (d) anaerobic digestion processes. The squares with different colors represent positive and negative correlation. The figure was illustrated with average values and standard error bans (the shaded area). (EDC: electron donating capacity; EAC: electron accepting capacity). (For interpretation of the references to color in this figure legend, the reader is referred to the Web version of this article.)

3. Results and discussion

3.1. Evolution of ETC of HA

In this study, the ETC of HA showed an increasing trend in both mesophilic and thermophilic AD. The ETC of HAs increased from 671 ± 15 and 774 ± 22 μmol gHA^{-1} to 1479 ± 26 and 1506 ± 13 μmol gHA^{-1} under mesophilic (Fig. 1 a) and thermophilic (Fig. 1 b) AD until day 25, respectively. Under mesophilic conditions, the EDC of HAs initially increased from 299 ± 17 to 762 ± 20 μmol gHA^{-1} and then gradually decreased to 718 ± 25 μmol gHA^{-1}. Under thermophilic conditions, the EDC initially increased from 327 ± 16 to 765 ± 21 μmol gHA^{-1} and then decreased to 745 ± 16 μmol gHA^{-1}. Moreover, the EAC of HAs under mesophilic conditions first increased and then decreased. The EAC value increased from 447 ± 15 to 761 ± 23 μmol gHA^{-1} over the entire thermophilic AD.

To investigate the contribution of structural characteristics to the differences in ETC of HAs during AD, the structural characteristics [including HIX, BIX, and contents of functional groups and chemical compositions] of HAs were first analyzed (Figs. S1 and S2, Table S1). Then, the detailed relationship between these structural indicators and the ETC of HA was further revealed (Fig. 1c and d). During mesophilic conditions (Fig. 1c), the ETC value was positively related to the HIX, element N content, and O-containing groups and negatively correlated with the BIX, element C content, element H content, and aromatic groups. This indicated that the N-containing moieties and O-containing groups were the main electron transfer functional groups of HA (He et al., 2014; Yang et al., 2016). Similarly, the HIX, element N content, aromatic groups, and O-containing groups contributed to the EAC value, while only the N content and O-containing groups contributed to the EDC value of HAs. This suggests that aromatic groups were also relevant to the EDC of HA formed under mesophilic conditions (Fellman et al., 2009; Tan et al., 2017; He et al., 2019). Unlike mesophilic conditions, the aromatic groups were great positively correlated with the EDC and ETC of HAs derived from the thermophilic AD (Fig. 1 d). This indicated that organic nitrogen, oxygen-containing groups, and aromatic groups were the main electron transfer functional moieties in HAs that contributed to the evolution of the ETC of HAs during AD (Zheng et al., 2019; He et al., 2019).

3.2. Interaction between microorganisms and ETC

The microbial communities, including bacterial and archaeal communities, were both determined using Illumina MiSeq sequencing (Fig. 2 a and b). The results show that *Fastidiosipila*, *Proteiniphilum*, *Mobilitalea*, *Tissierella*, *Caldicoprobacter* were the main bacterial communities, and the *Methanomassiliicoccus, Methanoculleus, Methanobacterium, Methanocorpusculum* were the main archaeal communities during the mesophilic AD (Fig. 2 a and b). Unlike the mesophilic condition, *Fastidiosipila, Proteiniphilum, Mobilitalea, Ruminiclostridium_1, Ruminococcaceae_NK4A214,* and *Ruminococcaceae_UCG_013* were the main bacterial communities and the *Methanothermobacter* was the main archaeal communities during the thermophilic AD. *Ruminiclostridium*, a typical flora in the hydrolysis stage of AD, exhibits high saccharolytic and proteolytic activities and is involved in carbohydrate hydrolysis and volatile fatty acid production (Zamanzadeh et al., 2016). Similarly, *Ruminococcaceae_NK4A214, Caldicoprobacter, Hydrogenispora, Mobilitalea,* and *Proteiniphilum* are involved in volatile fatty acid production during the acidogenic phase of AD (Huang et al., 2021). Moreover, *Methanomassiliicoccus, Methanothermobacter, Methanoculleus, Methanobacterium,* and *Methanocorpusculum* were the main archaeal communities, contributing to methane production in the methanogenic phase of AD (Magdalena et al., 2021).

The relationship between the evolution of the ETC of HAs and the functional genus species was analyzed separately under mesophilic and thermophilic AD conditions (Fig. 3 a and b). The results showed that ETC, including EDC and EAC, had a significantly positive correlation with the bacterial communities of *Ruminiclostridium, Ruminococcaceae, Caldicoprobacter, Hydrogenispora, Mobilitalea,* and *Proteiniphilum*. This result indicates that ETC may contribute to the reaction rate of the hydrolysis and acidogenic stages in AD. As the key step in AD, the hydrolysis phase is positively correlated with the respiration efficiency of microbial communities (Li et al., 2019a, 2019b). HAs, as electron acceptors, have the potential to promote the respiration of microbial communities and enhance the degradation of organic compounds (Bai et al., 2019). Likewise, in the acidogenic phase, HAs can act as electron acceptors and electron donors to promote the activities of acidifying bacteria and the conversion of soluble organic matter to volatile fatty acids (Liu et al., 2015). This result was consistent with the evolution of volatile fatty acids content (Fig. S3). Compared with the mesophilic condition, a higher content of volatile fatty acids was observed in the thermophilic condition, which may be attributed to the higher ETC of HA formed from the thermophilic condition (Fig. 1).

Principal component analysis showed that the ETCs of HAs had a significantly negative correlation with the archaeal communities of *Methanomassiliicoccus, Methanothermobacter, Methanoculleus, Methanobacterium, and Methanocorpusculum* (Fig. 3 b), indicating that ETC inhibited the activities of these archaeal communities in the

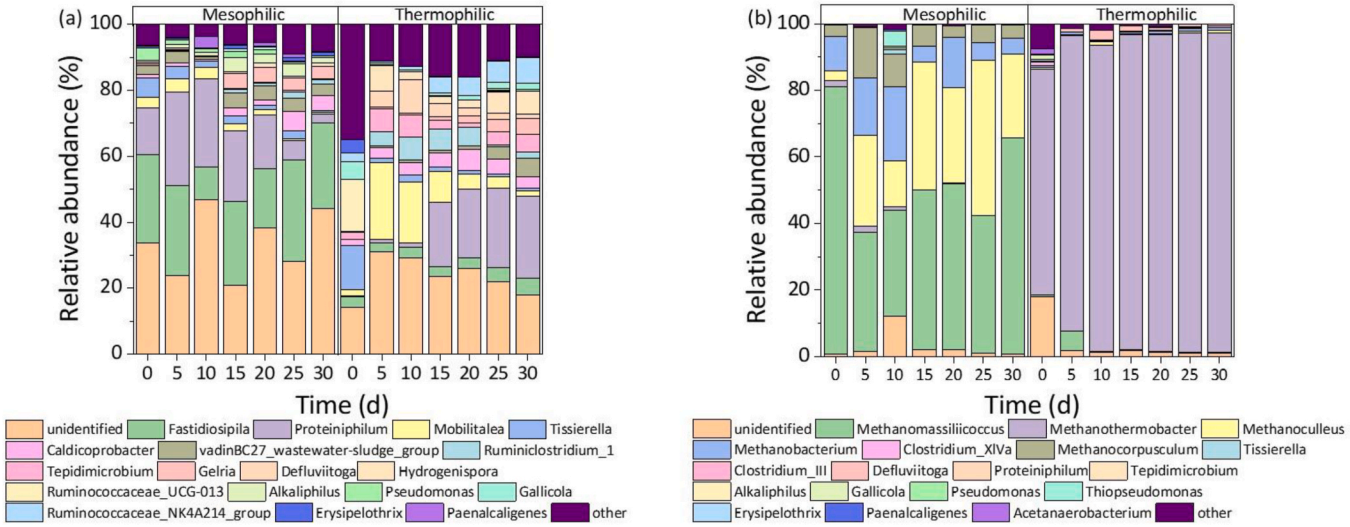

Fig. 2. Relative abundance of bacteria (a) and archaea (b) at genus level during the mesophilic and thermophilic stages of anaerobic digestion.

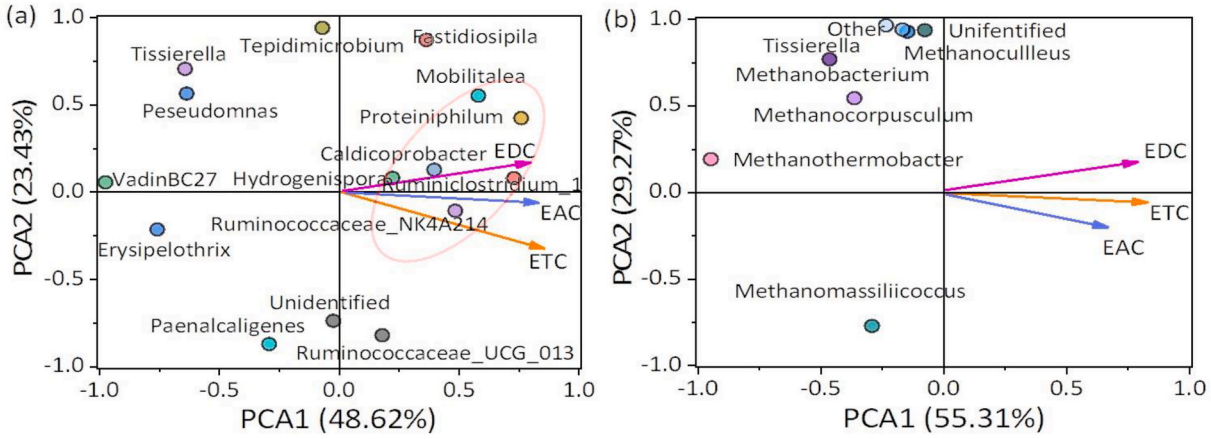

Fig. 3. Principal component analysis biplot showing the relationship between the evolution of bacteria (a), archaea (b), and electron transfer capacity during the mesophilic and thermophilic stages of anaerobic digestion. The percentages of two principal components (PCA 1 and PCA2) explained the contribution to the total variation.

methanogenic phase. This may be because HAs with a strong ETC compete with methanogens for electrons and may occupy a dominant position, thereby inhibiting the activities of methanogens (Zhao et al., 2017; Xi et al., 2016).

3.3. Dynamics of the key enzyme activities and their interactions with HA

Generally, AD performance is directly related to the activity of key enzymes produced by the microbial community in the hydrolysis, acidogenic, and methanogenic phases (Chen et al., 2021). To further explore the mechanisms of the effect of HAs on AD, the activities of key enzymes during mesophilic and thermophilic AD were monitored in this study (Fig. 4). During AD, proteins and polysaccharides are first hydrolyzed to amino acids and monosaccharides by hydrolytic enzymes, respectively (Li et al., 2019a, 2019b). As the key hydrolysis enzymes in the hydrolysis phase, the activities of amylase [1.63–1.85 (mesophilic) and 1.83–2.01 (thermophilic) U mL^{-1}] and protease [1.86–2.01 (mesophilic) and 1.82–1.95 (thermophilic) μmmol mL^{-1}] first increased and then decreased during mesophilic and thermophilic AD (Fig. 4 a and b).

After the hydrolysis phase, the generated amino acids were converted to short-chain fatty acids during the acidogenic phase by AK, BK, and PTA (Liu et al., 2015). The same trend of evolution was observed in the activities of AK, PTA, and BK in the acidogenic phase during mesophilic and thermophilic AD (Fig. 4 c, d, and e). The activity of F420-reducing hydrogenase, the key enzyme contributing to the transformation of short-chain fatty acids into methane in the methanogenic phase (Ye et al., 2016), decreased from 2.09 to 1.24 μmmol mL^{-1} during mesophilic AD and from 2.15 to 1.14 μmmol mL^{-1} during thermophilic AD (Fig. 4 f).

The relationship between the evolution of the ETC of HAs and the key enzyme activities in AD was determined using the co-occurrence network analysis. As shown in Fig. 5 a and b, in the visualized co-occurrence networks, the red and blue connections represent significantly positive and negative correlations between the measured parameters, respectively ($P < 0.05$). The results showed that the ETC of HAs had a significantly different influence on key enzyme activities during AD ($P < 0.05$). In detail, the ETC of HAs was significantly positively correlated with the activities of amylase and protease in the hydrolysis phase. This result indicated that the ETC of HAs promoted the activities of key enzymes in the hydrolysis phase.

Generally, HAs with a low ETC value interact with amylase and protease in the hydrolysis phase through hydrophobic and electrostatic forces, thereby inhibiting the activities of these key enzymes (Fernandes et al., 2015; Tang et al., 2018). However, with increasing ETC, the rejection from the negative charges of HAs would become stronger than their hydrophobic interactions with the enzymes. HAs work to release bound enzymes and promote enzyme activity to some extent (Li et al., 2019a, 2019b; Liu et al., 2015).

Similarly, the ETC of HAs promoted the activities of AK, BK, and PTA in the acidogenic phase. Generally, the activities of AK, BK, and PTA are hindered by "surplus electrons." For example, various electrons are produced in AD, but when microorganisms lack the electron transport system, "surplus electrons" are generated. The generated "surplus electrons" must be released to other substrates; otherwise, the activities of AK, BK, and PTA would be inhibited (Li et al., 2019a, 2019b). When HAs have a strong ETC, the functional groups of HAs (e.g., oxygen-containing groups) form good electron transfer chains and play a key role as electron transport agents in the acidogenic phase, thereby promoting the activities of acidifying enzymes and accelerating the reaction rate in the acidogenic phase.

In contrast, increased ETC inhibited the activity of F420-reducing hydrogenase in the methanogenic phase. This may be because HAs can directly accept electrons from acetate and prevent its conversion to methane, causing the blockade of normal methane pathway. Therefore, the surplus acetic acid could inhibit the activity of F420-reducing hydrogenase (Li et al., 2019a, 2019b; Khadem et al., 2017). Moreover, HAs may resemble a metabolic intermediate substance that promotes the metabolism of other syntrophic bacteria and cause the failure of methanogen competition in the AD system, which may lead to a reduction in F420-reducing hydrogenase activity (Azman et al., 2017; Dang et al., 2016).

Furthermore, the influence of HAs on the key enzyme activities was greater under thermophilic conditions than under mesophilic conditions (Fig. 5 a and b). This can be attributed to the stronger ETC of HAs formed under thermophilic conditions (Wang et al., 2021a, 2021b). Thus, as shown in Fig. 5 c, HAs promoted the hydrolysis and acidogenic phases, because the ETC of HAs can promote the activities of protease, amylase, AK, BK, and PTA. In the methanogenic phase, the ETC of HAs inhibited the activity of F420-reducing hydrogenase, thereby inhibiting the methanogenic phase.

4. Significance of this study

From the perspective of engineering applications, this study provides evidence-based knowledge to support the modulation of electron transfer capacity of humic acids, thereby improving the bio-waste treatment/management through anaerobic digestion processes. In the hydrolysis and acidification phases, the high electron transfer capacity of humic acid could benefit the activity of key enzymes (Fig. 5) and consequently enhance the degradation of the original bio-waste.

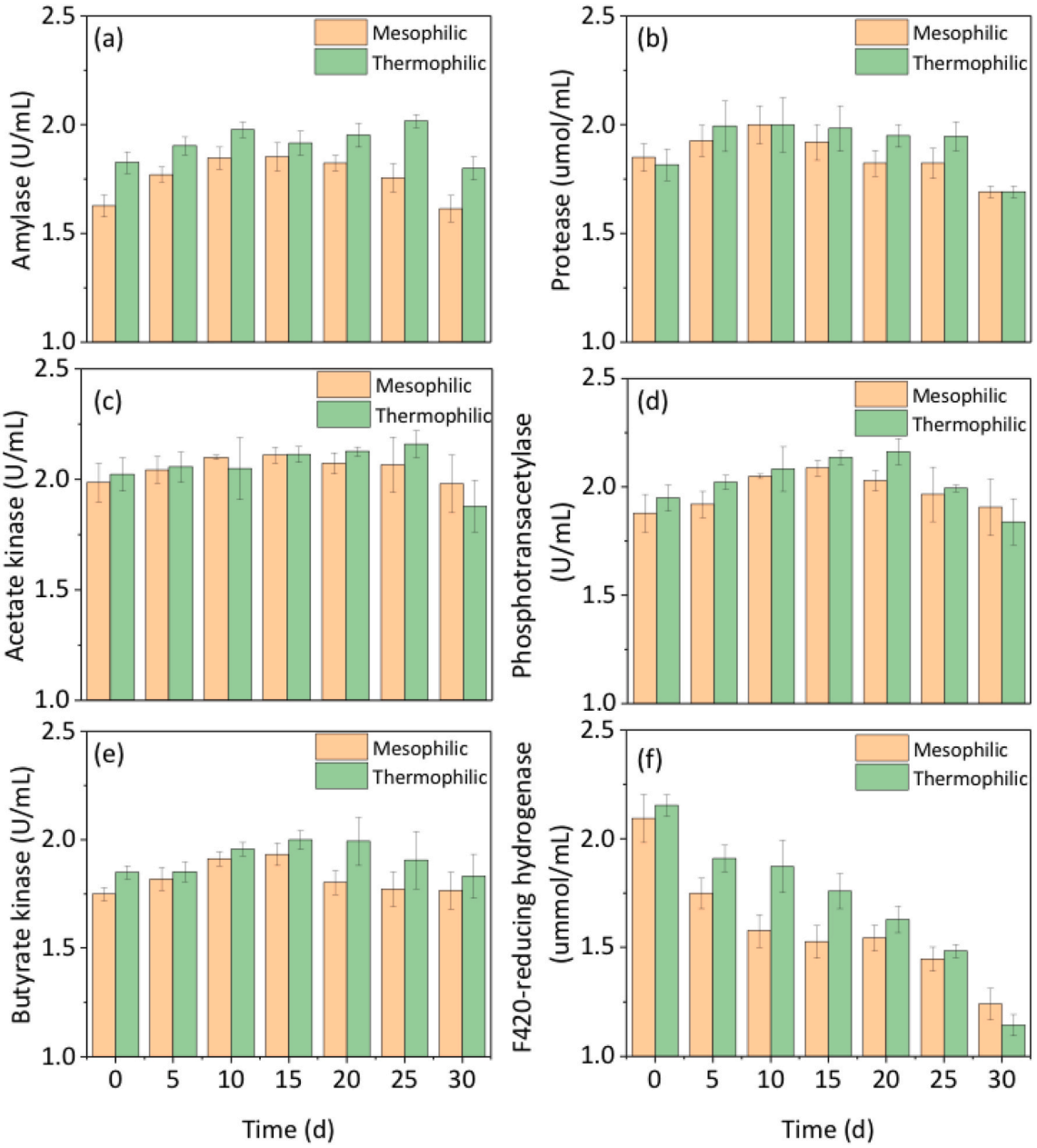

Fig. 4. Evolution of key enzyme activities of amylase (a), protease (b), acetate kinase (c), phosphotransacetylase (d), butyrate kinase (e), and F420-reducing hydrogenase (f), during the mesophilic and thermophilic anaerobic digestion.

Nevertheless, the high electron transfer capacity of humic acids could inhibit the activities of key enzymes in the methanogenic phase (Fig. 5). Therefore, a two-stage anaerobic digestion approach can be proposed to upgrade the efficiency of current anaerobic digestion plants. A higher operation temperature, e.g., under thermophilic condition (55 °C), could be conducted in the first stage reactor to increase the electron transfer capacity of the humic acid, thereby improving the hydrolysis and acidification of the bio-waste. In the second methanogenic stage, operation measures, e.g., the addition of trace elements (Fe^{2+} and Ni^{2+}), could be conducted to decrease the electron transfer capacity and increase methane production (Bi et al., 2019a, 2019b). Before the second stage methanogenic reactor, the digestate slurry with high humic acid content could also be taken out and reused for other purposes, e.g., organic fertilizer (Ye et al., 2019). Alternatively, the humic acid could be extracted through the membrane filtration method to reduce the sources of electron transfer shuttles (Xu et al., 2017), thus enhancing the methanogenic efficiency.

Notably, the current study focused on chicken manure as the anaerobic digestion feeding material. Different substrates, such as corn stover and waste-activated sludge, may lead to different key enzymes and microorganisms during the reaction. Thus, the interactions found in this study may be different when applying other substrates, which need further investigation. Moreover, the species and capabilities of various electron shuttles in the anaerobic digestion system were not covered by the current study and are worth studying further to have a better understanding of mechanisms. Nevertheless, this study opens up new insights towards developing the anaerobic digestion technology through understanding the effect of humic acid on the anaerobic digestion.

5. Conclusions

HAs with various ETCs formed during AD could significantly affect the microbial community structures and key enzyme activities, which play an important role in the overall AD performance in terms of

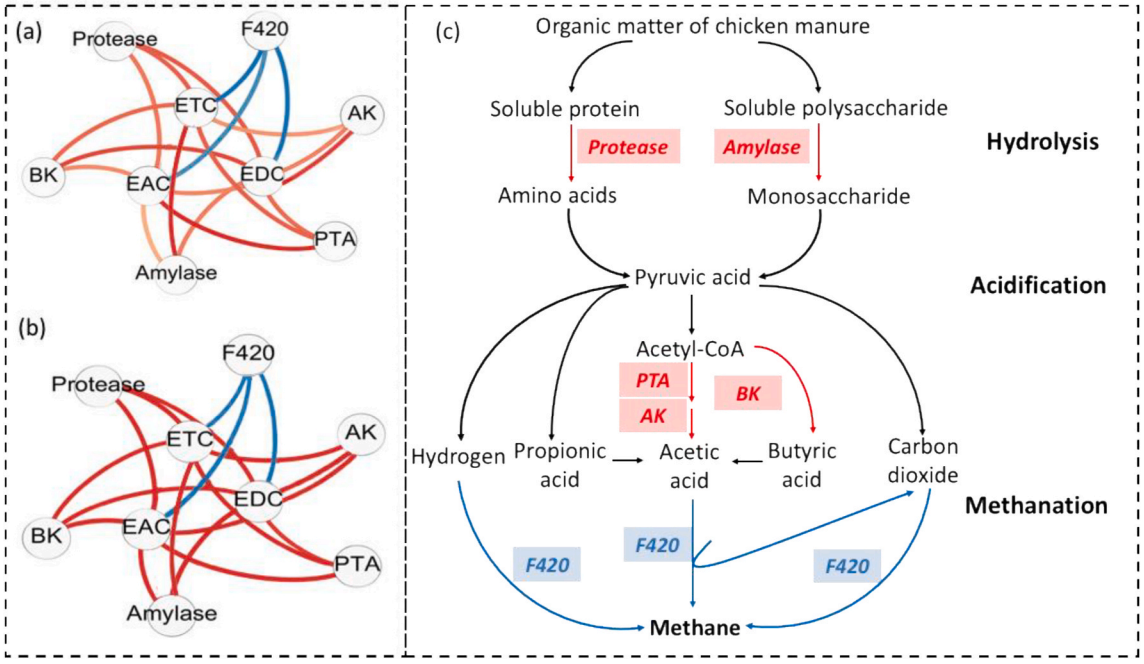

Fig. 5. Co-occurrence network of the electron transferring capacity (electron donating capacity and electron accepting capacity) indices indicating the activity of key enzymes during mesophilic (a) and thermophilic (b) anaerobic digestion. The nodes represent each parameter, and the connections (edges) represent significantly positive correlation (red) or negative correlation (blue). A more intense color indicates a stronger correlation. (c) Possible influence of humic acid on the anaerobic digestion system. The red label represents promotion, and the blue label represents inhibition. (AK: acetate kinase, BK: butyrate kinase, PTA: phosphotransacetylase, F420: F420-reducing hydrogenase). (For interpretation of the references to color in this figure legend, the reader is referred to the Web version of this article.)

methane production and bio-waste degradation. The high ETC of HAs promotes key enzyme activities and relevant microorganisms involved in hydrolysis and acidification reactions, while inhibiting methanogenic enzymes and microorganisms in the AD of chicken manure. These results provide new insights into the underlying mechanisms of the effect of HAs on methane generation in AD, which may benefit the further development of sustainable bio-waste management strategies.

Author contribution statement

Xiqing Wang: Experiment investigation, Sampling and analysis, Writing-Original draft preparation. Tao Lyu: Visualization, Methodology development. Renjie Dong: Conceptualization, Funding acquisition. Shubiao Wu: Writing- Reviewing and Editing, Project administration, Supervision, Funding acquisition.

Declaration of competing interest

The authors declare that they have no known competing financial interests or personal relationships that could have appeared to influence the work reported in this paper.

Acknowledgement

This work was financed by the National Natural Science Foundation of China (Grant No. 51650110489). We are also thankful to reviewers for their valuable suggestions to enhance the worth of this article.

Appendix A. Supplementary data

Supplementary data to this article can be found online at https://doi.org/10.1016/j.jenvman.2021.113914.

References

Azman, S., Khadem, A.F., Plugge, C.M., Stams, A.J.M., Bec, S., Zeeman, G., 2017. Effect of humic acid on anaerobic digestion of cellulose and xylan in completely stirred tank reactors: inhibitory effect, mitigation of the inhibition and the dynamics of the microbial communities. Appl. Microbiol. Biotechnol. 101, 889–901.

Allen, S., Kellermeyer, R., Stjernholm, R., Wood, H., 1964. Purification and properties of enzymes involved in the propionic acid fermentation. J. Bacteriol. 87, 171–187.

Aeschbacher, M., Sander, M., Schwarzenbach, R.P., 2010. Novel electrochemical approach to assess the redox properties of humic substances. Environ. Sci. Technol. 44, 87–93.

Bi, S., Westerholm, M., Qiao, W., Mahdy, A., Xiong, L., Yin, D., Fan, R., Dach, J., Dong, R., 2019a. Enhanced methanogenic performance and metabolic pathway of high solid anaerobic digestion of chicken manure by Fe^{2+} and Ni^{2+} supplementation. Waste Manag. 94, 10–17.

Bai, Y.N., Wang, X.N., Wu, J., Lu, Y.Z., Fu, L., Zhang, F., Lau, T.C., Zeng, R.J., 2019. Humic substances as electron acceptors for anaerobic oxidation of methane driven by ANME-2d. Water Res. 164, 114935.

Bi, S., Qiao, W., Xiong, L., Ricci, M., Adani, F., Dong, R., 2019b. Effects of organic loading rate on anaerobic digestion of chicken manure under mesophilic and thermophilic conditions. Renew. Energy 139, 242–250.

Chen, H., Tang, M., Yang, X., Tsang, Y.F., Wu, Y., Wang, D., Zhou, Y., 2021. Polyamide 6 microplastics facilitate methane production during anaerobic digestion of waste activated sludge. Chem. Eng. J. 408, 127251.

Chen, X., Liu, R., Hao, J., Li, D., Wei, Z., Teng, R., Sun, B., 2019. Protein and carbohydrate drive microbial responses in diverse ways during different animal manures composting. Bioresour. Technol. 271, 482–486.

Dang, Y., Lei, Y., Liu, Z., Xue, Y., Sun, D., Wang, L.Y., Holmes, D.E., 2016. Impact of fulvic acids on bio-methanogenic treatment of municipal solid waste incineration leachate. Water Res. 106, 71–78.

Fernandes, T.V., Lier, J.B., Zeeman, G., 2015. Humic acid-like and fulvic acid- like inhibition on the hydrolysis of cellulose and tributyrin. Bioenergy Res 8, 821–831.

Fellman, J.B., Miller, M.P., Cory, R.M., Amore, D.V., White, D., 2009. Characterizing dissolved organic matter using PARAFAC modelling of fluorescence spectroscopy: a comparison of two models. Environ. Sci. Technol. 43, 6228–6234.

Guo, X., Liu, H., Wu, S., 2019. Humic substances developed during organic waste composting: formation mechanisms, structural properties, and agronomic functions. Sci. Total Environ. 662, 501–510.

He, X.S., Xi, B.D., Cui, D.Y., Liu, Y., Tan, W.B., Pan, H.W., Li, D., 2014. Influence of chemical and structural evolution of dissolved organic matter on electron transfer capacity during composting. J. Hazard Mater. 268, 256–263.

He, X.S., Yang, C., You, S.H., Zhang, H., Xi, B.D., Yu, M.D., Liu, S.J., 2019. Redox properties of compost-derived organic matter and their association with polarity and molecular weight. Sci. Total Environ. 665, 920–928.

Huang, S., Shen, M., Ren, Z.J., Wu, H., Yang, H., Si, B., Lin, J., Liu, Z., 2021. Long-term in situ bioelectrochemical monitoring of biohythane process: metabolic interactions and microbial evolution. Bioresour. Technol. 332, 125119.
Khadem, A.F., Azman, S., Plugge, C.M., Zeeman, G., Lier, J.B., Stams, A.J.M., 2017. Effect of humic acids on the activity of pure and mixed methanogenic cultures. Biomass Bioenergy 99, 21–30.
Li, J., Hao, X., Loosdrecht, C.M.M., Luo, Y., Cao, D., 2019a. Effect of humic acids on batch anaerobic digestion of excess sludge. Water Res. 155, 431–443.
Li, J., Hao, X., Loosdrecht, C.M.M., Yu, J., Liu, R., 2019b. Adaptation of semi-continuous anaerobic sludge digestion to humic acids. Water Res. 161, 329–334.
Li, H., Li, Y., Jin, Y., Zou, S., Li, C., 2014. Recovery of sludge humic acids with alkaline pretreatment and its impact on subsequent anaerobic digestion. J. Chem. Technol. Biotechnol. 89, 707–713.
Liu, K., Chen, Y., Xiao, N., Zheng, X., Li, M., 2015. Effect of humic acids with different characteristics on fermentative short-chain fatty acids production from waste activated sludge. Environ. Sci. Technol. 49, 4929–4936.
Lyu, T., Zhang, L., Xu, X., Arias, C.A., Brix, H., Carvalho, P.N., 2018. Removal of the pesticide tebuconazole in constructed wetlands: design comparison influencing factors and modelling. Environ. Pollut. 233, 71–80.
Magdalena, J.A., Greses, S., González-Fernández, C., 2021. Valorisation of bioethanol production residues through anaerobic digestion: methane production and microbial communities. Sci. Total Environ. 772, 144954.
Provenzano, M.R., Malerba, A.D., Pezzolla, D., Gigliotti, G., 2014. Chemical and spectroscopic characterization of organic matter during the anaerobic digestion and successive composting of pig slurry. Waste Manag. 34 (3), 653–660.
Rehman, K., Cai, M., Xiao, X., Zheng, L., Wang, H., Soomro, A.A., Zhou, Y., Li, W., Yu, Z., Zhang, J., 2017. Cellulose decomposition and larval biomass production from the co-digestion of dairy manure and chicken manure by mini-livestock (Hermetia illucens L.). J. Environ. Manag. 196, 458–465.
Rehman, K., Rehman, R.U., Somroo, A.A., Cai, M., Zheng, L., Xiao, X., Rehman, A.U., Rehman, A., Tomberlin, J.K., Yu, Z., Zhang, J., 2019. Enhanced bioconversion of dairy and chicken manure by the interaction of exogenous bacteria and black soldier fly larvae. J. Environ. Manag. 237, 75–83.
SCA (Standing Committee of Analysts), 2011. Methods for the Examination of Waters and Associated Materials, Bluebook 236 British Standards. Environmental Policy and Law.
Tang, Y., Li, X., Dong, B., Huang, J., Wei, Y., Dai, X., Dai, L., 2018. Effect of aromatic repolymerization of humic acid-like fraction on digestate phytotoxicity reduction during high-solid anaerobic digestion for stabilization treatment of sewage sludge. Water Res. 143, 436–444.
Tan, W., Xi, B., Wang, G., Jiang, J., He, X., Mao, X., Gao, R., Huang, C., Zhang, H., Li, D., Jia, Y., Yuan, Y., Zhao, X., 2017. Increased electron-accepting and decreased electron-donating capacities of soil humic substances in response to increasing temperature. Environ. Sci. Technol. 51, 3176–3186.
Trevors, J.T., 1984. Dehydrogenase activity in soil: a comparison between the INT and TTC assay. Soil Biol. Biochem. 16, 673–674.
Wang, X., Lyu, T., Dong, R., Liu, H., Wu, S., 2021a. Dynamic evolution of humic acids during anaerobic digestion: exploring an effective auxiliary agent for heavy metal remediation. Bioresour. Technol. 320, 124331.
Wang, X., Muhmood, A., Lyu, T., Dong, R., Liu, H., Wu, S., 2021b. Mechanisms of genuine humic acid evolution and its dynamic interaction with methane production in anaerobic digestion processes. Chem. Eng. J. 408, 127322.
Xiao, X., Xi, B.D., He, X.S., Zhang, H., Li, D., Zhao, X.Y., Zhang, X.H., 2019. Hydrophobicity-dependent electron transfer capacities of dissolved organic matter derived from chicken manure compost. Chemosphere 222, 757–765.
Xi, B., Zhao, X., He, X., Huang, C., Tan, W., Gao, R., Zhang, H., Li, D., 2016. Successions and diversity of humic-reducing microorganisms and their association with physical-chemical parameters during composting. Bioresour. Technol. 219, 204–211.
Xu, Y., Chen, C., Li, X., Lin, J., Liao, Y., Jin, Z., 2017. Recovery of humic substances from leachate nanofiltration concentrate by a two-stage process of tight ultrafiltration membrane. J. Clean. Prod. 161, 84–94.
Yang, Z., Du, M., Jiang, J., 2016. Reducing capacities and redox potentials of humic substances extracted from sewage sludge. Chemosphere 144, 902–908.
Ye, R., Keller, J.K., Jin, Q., Bohannan, B.J.M., Bridgham, S.D., 2016. Peatland types influence the inhibitory effects of a humic substance analog on methane production. Geoderma 265, 131–140.
Ye, W., Liu, H., Jiang, M., Lin, J., Ye, K., Fang, S., Xu, Y., Zhao, S., Bruggen, B.V.D., He, Z., 2019. Sustainable management of landfill leachate concentrate through recovering humic substance as liquid fertilizer by loose nanofiltration. Water Res. 157, 555–563.
Zhao, X., He, X., Xi, B., Gao, R., Tan, W., Zhang, H., Huang, C., Li, D., Li, M., 2017. Response of humic-reducing microorganisms to the redox properties of humic substance during composting. Waste Manag. 70, 37–44.
Zamanzadeh, M., Hagen, L.H., Svensson, K., Linjordet, R., Horn, S.J., 2016. Anaerobic digestion of food waste-effect of recirculation and temperature on performance and microbiology. Water Res. 96, 246–254.
Zhao, X., Tan, W., Peng, J., Dang, Q., Zhang, H., Xi, B., 2020. Biowaste-source-dependent synthetic pathways of redox functional groups within humic acids favoring pentachlorophenol dechlorination in composting process. Environ. Int. 135, 105380.
Zheng, X., Liu, Y., Fu, H., Qu, X., Yan, M., Zhang, S., Zhu, D., 2019. Comparing electron donating/accepting capacities (EDC/EAC) between crop residue-derived dissolved black carbon and standard humic substances. Sci. Total Environ. 673, 29–35.
Zhang, X., Yan, S., Tyagi, R.D., Surampalli, R.Y., Valero, J.R., 2014. Ultrasonication aided in-situ transesterification of microbial lipids to biodiesel. Bioresour. Technol. 169, 175–180.